Microbubble skin friction reduction on an axisymmetric body under the influence of applied axial pressure gradients

H. Clark III and S. Deutsch
Applied Research Laboratory, Pennsylvania State University, P. O. Box 30, State College, Pennsylvania 16804

(Received 29 March 1991; accepted 19 August 1991)

The influence of both a favorable and an adverse applied axial pressure gradient on microbubble-induced skin friction reduction was examined. An 87 mm diameter, 632 mm long model equipped with a 273 mm long cylindrical force balance was employed. Experiments were carried out in a 305 mm diameter water tunnel, at free-stream speeds of 4.6, 7.6, 10.7, 13.7, and 16.8 m/sec. Air was injected at rates as high as 12×10^{-3} m^3/sec. Measurement of the static pressure along the body with gas injection demonstrated that gas injection did not alter the pressure gradient and that the flow remained axisymmetric. Reductions in skin friction for the zero pressure gradient case agreed well with the earlier results of Deutsch and Castano [Phys. Fluids **29**, 3590 (1986)]. The adverse-gradient induced separation of the boundary layer for speeds at and above 7.6 m/sec, for air injection rates in excess of 5.0×10^{-3} m^3/sec. The favorable gradient strongly inhibited the drag reduction mechanism [47].

I. INTRODUCTION

The injection of gas to form microbubbles in a liquid turbulent boundary layer has been shown in many studies[1-10] to reduce skin friction drag. Most of the experimental work done to date has been performed in flat-plate geometries.[2-8] Several analytical/computational studies[11,12] have also been made in an attempt to provide a sensible model for the phenomenon. On the basis of most of the experimental data, it is believed that the presence of microbubbles in the very near-wall region (buffer layer) tends to destroy the turbulent production scales there, effectively enlarging the viscous sublayer and reducing the velocity gradient at the wall. An alternate interpretation in which the mixing length is changed as a function of gas concentration, is given by Legner.[11] A comprehensive review by Merkle and Deutsch[13] is now available.

The present study extends the experiments of Deutsch and Castano[9] and Deutsch and Pal,[10] in which the microbubble phenomenon was examined on an axisymmetric shape. In the following, then, we present a synopsis of these earlier studies. All of these experiments were conducted in the 305 mm diameter water tunnel at the Applied Research Laboratory of Pennsylvania State University using an 87 mm diameter axisymmetric model (cf. Fig. 1).

Deutsch and Castano[9] measured the integrated skin friction and the static pressure gradient on the tunnel wall in the presence of gas injection. They found that, although the maximum level of overall skin friction reduction was about the same as for the flat-plate geometries, the drag reduction peaked at higher rather than the lower tunnel speeds. Reductions of as much as 80% were observed. Helium seemed to be somewhat more effective in reducing drag than was air. Static pressure measurements, made on the wall of the tunnel, showed that the injection of gas neither changed the pressure gradient nor the axial symmetry of the flow field. LDV measurements, which were used to determine the friction velocity u^* at three locations on the balance section, agreed, when compared with balance measurements, to within 10%.

Deutsch and Pal[10] attempted to clarify the differing drag reduction versus tunnel speed characteristics of the axisymmetric shape relative to flat plates by looking at the local reduction of shear stress. They used an array of 12 hot film probes, which were symmetrically mounted on the balance section at the three streamwise locations at which LDV profiles had been made. Using the film probes and flow visualization, they determined that the flow field at speeds above 10.7 m/sec behaved very much like the flat-plate flow field. That is, the influence of buoyancy, which acted to move the entire gas cloud up, gradually decreased as the free-stream speed increased. In general, the gas flow was slowly transported from the bottom to the top of the model, resulting eventually, in more drag reduction at the top. As in the flat-plate flows, the persistence of the phenomenon was found to last some 30 to 40 boundary layer thicknesses. The influence of the bubbles on the wall shear stress statistics was also found to be the same as that observed for a flat plate.[14] For speeds below about 10.7 m/sec, however, the flow was dominated by a double-vortex structure that entrained and removed bubbles from the bottom and sides of the model and moved them to the top. The vortex structure appeared abruptly as the air flow was increased at a constant tunnel speed. The loss of bubbles from the boundary layer was found to account for the loss of drag reduction effectiveness at the low speeds.

In the current study, we extend the measurement set of Deutsch and Castano[9] and Deutsch and Pal[10] by considering the influence of applied axial pressure gradients on the drag reduction phenomenon.

II. EXPERIMENTAL APPARATUS AND PROCEDURE

The experiments were performed in the same 305 mm diameter water tunnel at ARL Penn State that was used by Deutsch and Castano[9] and Deutsch and Pal.[10] The model used in the current investigation was also essentially the same, differing only in that it had a longer injection section (40 mm to 6.35 mm) and a correspondingly shorter nose to

 0899-8213/91/122948-07$02.00

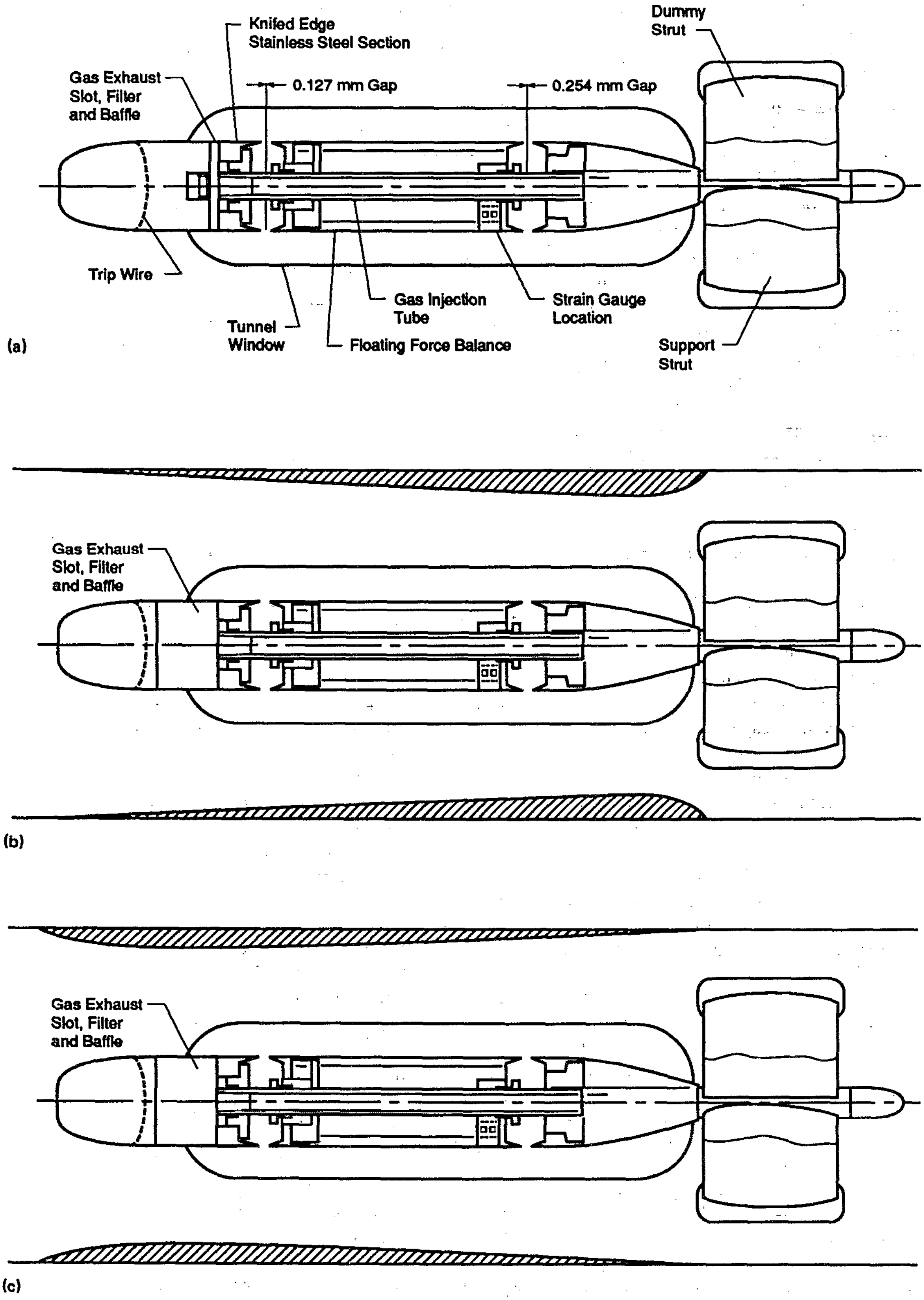

FIG. 1. Schematic of the 87 mm diameter axisymmetric skin friction model. (a) The narrow injector is shown, while (b) and (c) show the wider injector in favorable and unfavorable pressure gradients, respectively.

preserve the overall length of the model. The injection section, which was constructed from the same 5 μm porous plastic filter material used in the earlier work, was located 104 mm downstream of the nose of the model. The longer injection section was employed in an attempt to improve the symmetry of the injected gas flow. The shorter injectors had a tendency to clog with time and often had to be replaced during the course of an experiment. We had hoped that the longer injection section would maintain gas symmetry longer. Such an improvement was not observed. We also note that some unpublished studies[15] indicate that the injection region may take a drag penalty, so that maintaining as short an injection section as practical is probably desirable. A schematic of the original model is shown in Fig. 1(a), while the current model, with a longer injection length is represented by Figs. 1(b) and 1(c). The mounting of the model in the tunnel was accomplished as in the earlier work. A 0.35 mm diameter trip wire was again placed at a distance of 46 mm from the nose of the body. A rotameter, with a pressure gauge at its inlet, was used to monitor the gas flow rate. Air was the only gas tested.

Integrated skin friction drag was measured using a force balance. The balance and adjoining sections were knife-edged in an effort to reduce pressure effects. As in the earlier axisymmetric body studies, an extremely stiff shear member was used in the force balance in order to minimize the distance travelled by the balance, in this way minimizing the gap widths. Using this shear gauge the balance gaps could be maintained at 0.127 mm and 0.254 mm at the upstream and downstream edges of the balance, respectively. The motion of the balance at maximum load was estimated to be no larger than 2.5 μm. Measurements of the skin friction drag were taken for the zero, favorable, and adverse pressure gradients at nominal tunnel speeds of 4.6, 7.6, 10.7, 13.7, and 16.8 m/sec.

LDV surveys of the gas-free boundary layers, for each of the pressure gradients, were conducted using an 8 W argon-ion laser, standard TSI optics in backscatter, and a 1980 counter processor. A small amount of 1.5 μm silicon carbide particles was added to the tunnel as seed. The data were stored and reduced on an IBM AT-PC. Velocity profiles were measured at three axial locations on the balance—210, 337, and 463 mm from the nose of the body—at tunnel speeds of 4.6 and 10.7 m/sec. One thousand data points were taken at each location in the boundary layers. A software program described by Zierke and Deutsch[16] was used to calculate a number of the boundary layer parameters. Results of the surveys are given in Table I.

Although Deutsch and Castano[9] showed that the injection of bubbles did not alter the axial pressure gradient or the axial symmetry of the flow by measuring the pressure on the tunnel walls, we felt that because the balance section would be operating in a nonzero pressure gradient it was essential to recheck these results. To this end, the force balance was replaced with a section that contained 38 static pressure taps. Fourteen taps were installed in the axial direction at the top of the model, while eight taps were installed on each of the sides and at the bottom of the model. The taps on the top of the model were separated by 22.5 mm; while the separation of those on the side was proportionately larger. The first set of taps, at the top, bottom, and sides, was located immediately upstream of the upstream balance gap. Pressure was measured using Foxboro 0–50 psi pressure transducers. Linearity of these transducers is excellent and the transducer accuracy is estimated to be to within $\pm$ 0.02 psi. The transducers were calibrated using an Ametek deadweight tester. The 38 static pressure lines were removed from the tunnel by using a specially designed fitting at the intersection of a support strut with the tunnel wall. This could not be done for the pressure gradient cases because of the possibility of compromising the thin liner, so that these static pressure measurements would only be taken for the zero pressure gradient case. The data were collected and reduced on a VAX 11/780 computer.

TABLE I. Characteristic boundary layer parameters for each pressure gradient.

Location[a] (mm)	U_∞ (m/sec)	δ (mm)	δ^* (mm)	θ (mm)	Re_θ	u^* (m/sec)
		Zero pressure gradient				
164	4.94	4.67	0.869	0.560	2754	0.190
164	11.03	5.44	0.954	0.642	7083	0.389
291	4.80	6.59	1.09	0.740	3545	0.191
291	10.97	7.07	1.11	0.793	8699	0.402
417	4.84	7.93	1.26	0.877	4242	0.191
417	11.10	8.51	1.19	0.879	9758	0.412
		Favorable pressure gradient				
164	5.17	4.37	0.752	0.504	3884	0.243
164	12.35	4.63	0.754	0.520	6410	0.463
291	5.59	5.86	0.822	0.587	3290	0.233
291	13.00	5.74	0.782	0.580	7536	0.500
417	5.89	6.65	0.884	0.659	3884	0.243
417	13.70	6.40	0.822	0.607	8305	0.522
		Adverse pressure gradient				
164	5.84	4.71	0.900	0.610	3563	0.217
164	13.25	4.63	0.834	0.572	7567	0.464
291	5.50	6.68	1.12	0.802	4406	0.212
291	12.88	6.56	1.01	0.736	9476	0.465
417	5.22	8.49	1.35	0.984	5142	0.201
417	12.44	8.36	1.27	0.932	11598	0.443

[a] Measured from trip wire.

To produce the favorable and adverse axial pressure gradients, two clear acrylic, axisymmetric liners were constructed for this tunnel test section. This choice of liner material permitted LDV measurements and visual inspection of the flow. The liner that generated the favorable pressure gradient went from a minimum thickness of 0.1 mm at the nose of the body, to a maximum thickness of 16.5 mm at the body's downstream end. This liner caused an approximate 28% increase in the dynamic pressure over the length of the body. To produce the adverse gradient, the liner first narrowed the tunnel area to 86% of its initial open area (a thickness of 11 mm) and then gradually diverged to a thickness of 2.6 mm at the downstream end of body. The minimum tunnel area occurred at a distance of 109.7 mm from the nose of the body. This liner caused an approximate 20% decrease in dynamic pressure. A schematic of the model and liner for the favorable pressure gradient is shown in Fig. 1(b) and for the unfavorable gradient in Fig. 1(c). Both the measured and calculated velocity distributions as a function of the axial distance, for each of the liners, are given for a nominal free-stream speed of 10.7 m/sec in Fig. 2. The calculated values shown are the result of a simple one-dimensional calculation. The location of the force balance is also shown in the figure.

Two parameters that are commonly used to describe the strength of a pressure gradient are, from Refs. 17 and 18, respectively,

$$K_u = \left(\frac{\nu}{U_\infty^2}\right)\frac{dU_\infty}{dx},$$

and

$$K_p = \left(\frac{\nu}{\rho u^{*3}}\right)\frac{\partial P}{\partial x},$$

where ν is the kinematic viscosity, U_∞ is the free-stream velocity, and ρ is the density of the liquid. Using measurements taken with the LDV at tunnel velocities of 4.6 and 10.7 m/sec and the properties of the gas-free liquid, we found that the experimental values of these parameters ranged, for the favorable pressure gradient, from 2.8×10^{-8} to 10.7×10^{-8} for K_u and from 4.9×10^{-4} to 11×10^{-4} for K_p. These values are very much smaller than those required to relaminarize the flow.[19] In fact, when compared to, say, the experimental data of Kline *et al.*[17] we find that the applied gradient is very weak. A comparably weak effect is noted for the adverse gradient for which K_u ranged from -1.8×10^{-8} to -9×10^{-8}, while K_p ranged from -4.1×10^{-4} to -16.7×10^{-4}.

The usefulness of these parameters in describing the dynamics of inhomogeneous two-phase fluids is not apparent. The variation of gas concentration and the corresponding variation of mixture density and viscosity across the boundary layer imply that the parameters must be functions of the distance from the wall. Madavan *et al.*[12] have shown that, for a gas volume fraction of 0.5, the mixture viscosity may be some 40 times higher than that of water. The parameter K_u then may be some 40 times higher than for the no-gas case, locally. The parameter K_p, which is a function of the shear velocity, may be even more strongly affected. This is particularly true for the adverse pressure gradient case in which u^* may drop to 20% of its no-gas value.

It seems clear in any event, that these parameters can only be used with a good deal of caution. It is likely that the effect of the pressure gradient on the low-momentum fluid in the near-wall region will be different from its effect on the higher-momentum fluid in the outer region. In particular, it is reasonable to expect then, that the trajectory of the bubble cloud will be different with and without pressure gradient.

III. RESULTS

Typical graphs of the coefficient of pressure and the velocity ratio are presented in Fig. 3 as a function of axial distance downstream of the trip wire. Several gas injection rates are shown. The drop in velocity associated with the last axial tap is caused by a narrowing of the body just downstream of that tap. The figures show that variations in both velocity and pressure are small, with no systematic variation with changes in injected gas flow. These results indicate, in support of the work of Deutsch and Castano,[9] that gas injection does not have a measurable effect on the pressure gradient or on the symmetry of the flow.

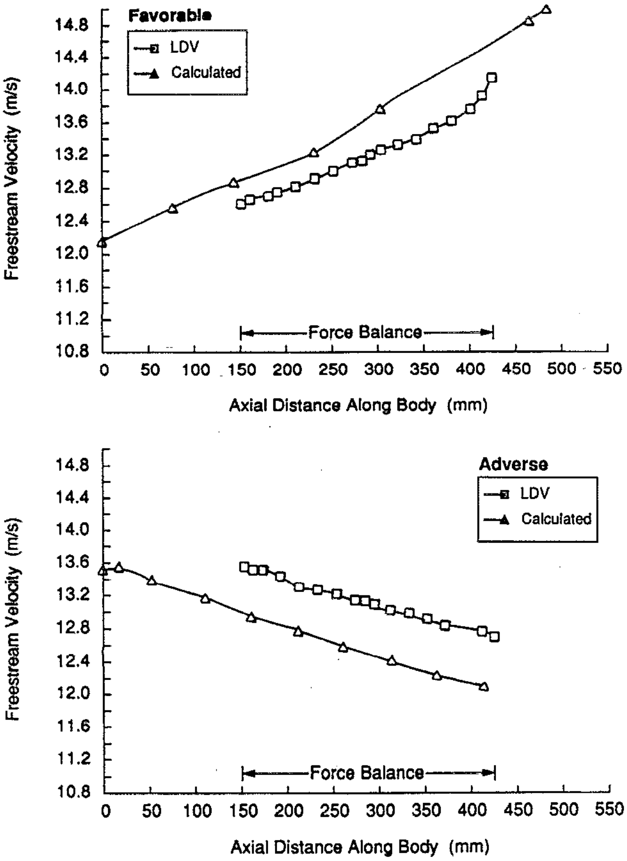

FIG. 2. Dynamic pressure versus axial distance for favorable and adverse pressure gradients.

Boundary layer parameters are given in Table I for each pressure gradient. These data are a result of LDV surveys that could only be made for the case without gas injection. The boundary layer thicknesses found in the present study, for the zero pressure gradient case, are on the average about 12% greater than those found by Deutsch and Castano.[9] This was possibly due to an increase in the surface roughness over a portion of the model because of the much wider injection section used in the current work.

Inner variable plots are shown for each of the pressure gradients in Fig. 4. These data were used to calculate the friction velocity by fitting each of the curves to the law of the wall. The resulting values were then integrated and compared to the force balance data. These two measurements agreed in every case to within 10%.

Results from the force balance measurements for all three gradients are presented in Figs. 5–9. The data set agrees very well with that presented for the zero pressure gradient case by Deutsch and Castano.[9] For this range of gas injection rates, a maximum drag reduction of 80% is found

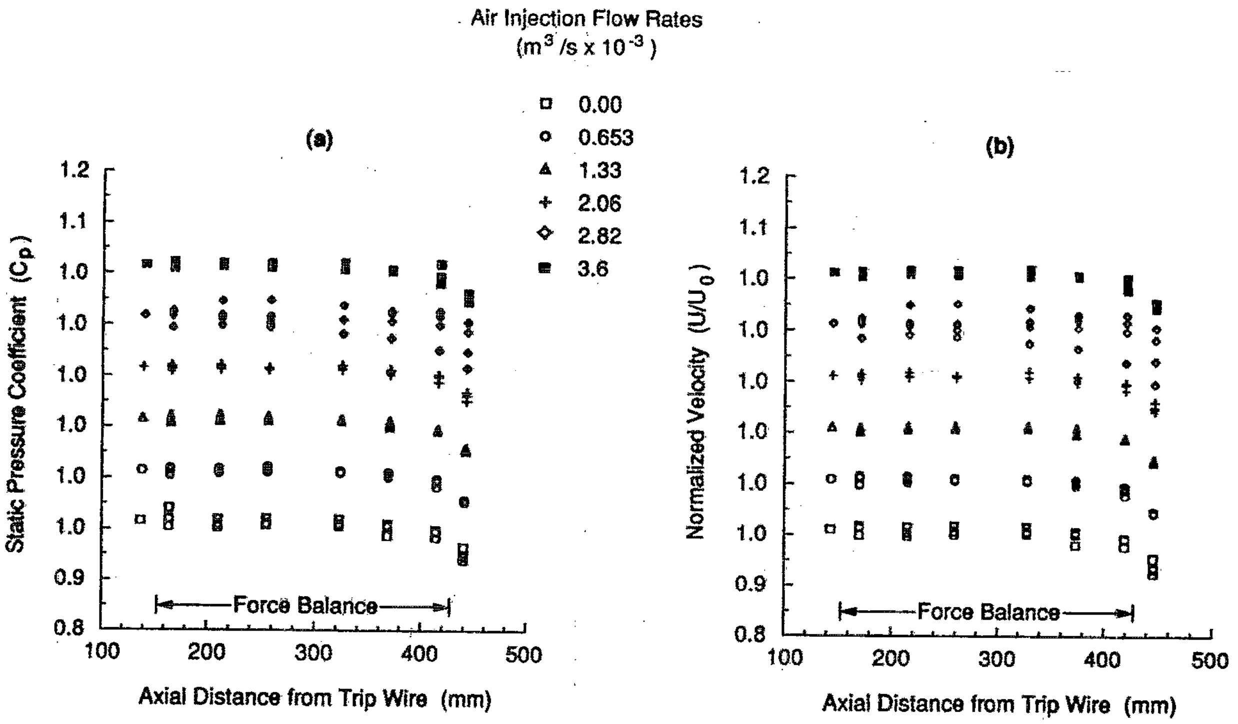

FIG. 3. Static pressure coefficient (a) and normalized velocity distribution (b) with air injection at a free-stream velocity of 16.8 m/sec. Note the shifted axes for C_p and U/U_0.

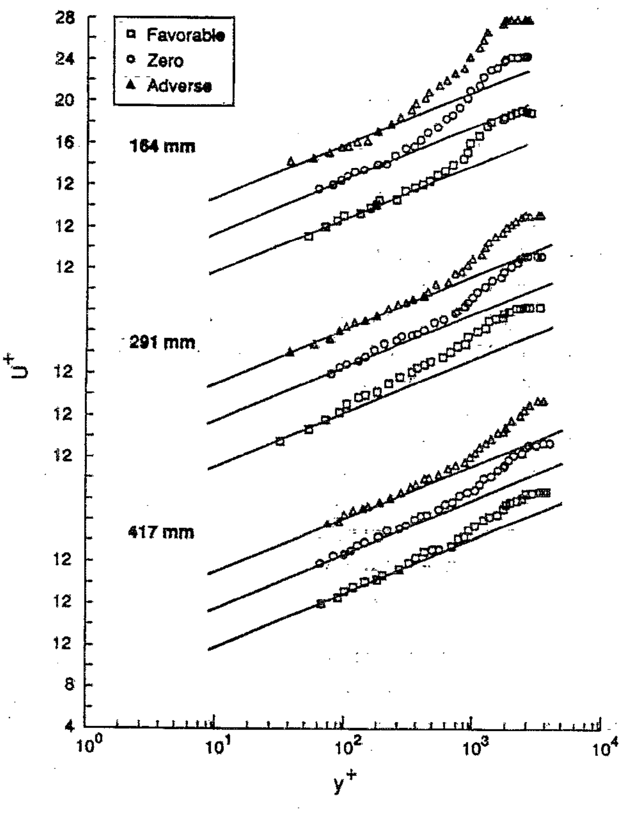

FIG. 4. Normalized LDV profiles in inner variables for each pressure gradient at a nominal flow velocity of 10.7 m/sec. Note the shifted axis for u^+.

for a tunnel speed of 10.7 m/sec. Drag reduction at speeds below 10.7 m/sec is limited by the onset of the buoyant instability discussed by Deutsch and pal,[10] while drag reduction at speeds above 10.7 m/sec is limited by the decreasing ratio of gas to total volume in the boundary layer with increasing tunnel speed. Merkle and Deutsch[13] have shown that drag reduction, in the absence of strong buoyant effects, increases with increases in the amount of gas volume flow rate to the total volume flow rate in the boundary layer.

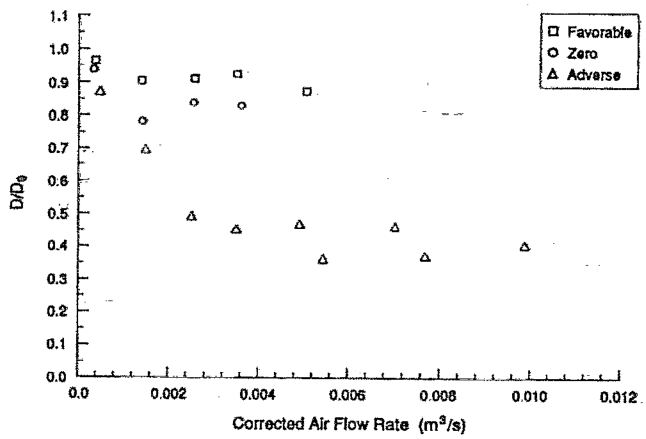

FIG. 5. Drag ratio versus corrected air flow rate for each pressure gradient at $U_\infty = 4.6$ m/sec.

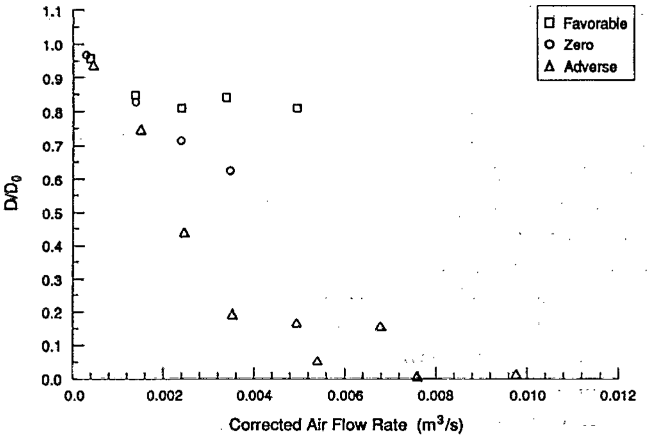

FIG. 6. Drag ratio versus corrected air flow rate for each pressure gradient at $U_\infty = 7.6$ m/sec.

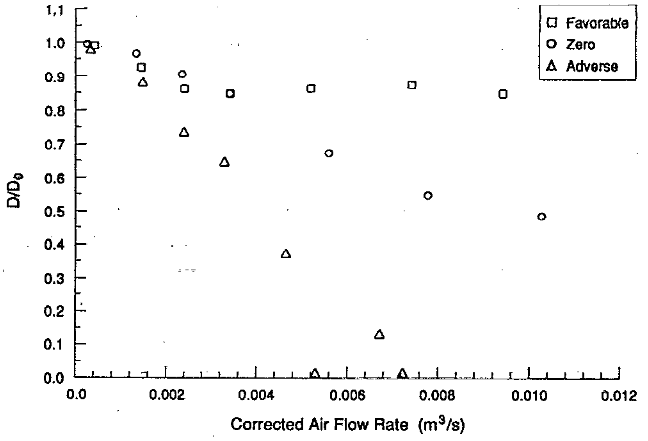

FIG. 8. Drag ratio versus corrected air flow rate for each pressure gradient at $U_\infty = 13.7$ m/sec.

It is evident from the figures that the presence of a favorable gradient is somehow inhibiting the amount of drag reduction. None of the combinations of gas injection rate or tunnel speed tested resulted in drag reduction in excess of 20%. The result is quite surprising as neither the inner nor outer scales of the boundary layer were dramatically changed by the favorable gradient. Values of the pressure gradient parameters, when calculated from the properties of the gas-free liquid, also suggest only a weak influence. The reason that the favorable gradient strongly inhibits the drag reduction mechanism is not yet understood.

The results for the flow with adverse pressure gradient are equally dramatic. Contrary to the zero pressure gradient case, there is substantial drag reduction, of nearly 60%, at the lowest speed of 4.6 m/sec. The adverse gradient appears to inhibit the formation of the buoyant instability. At freestream velocities of 7.6 m/sec and above, the introduction of gas flow rates higher than about 5×10^{-3} m^3/sec resulted in separation of the two-phase, gas–liquid boundary layer. This separation was noted both visually and by the balance results going to zero. The data suggest that the gas flow rate at which separation first occurs is not a strong function of the tunnel speed. It is important to note here, that the separation of the boundary layer was easily visualized in the adverse gradient case with the bubbles clearly moving downstream. Such visualization agreed well with the balance results and provided a test of the accuracy of the balance measurements in a pressure gradient.

Very large reductions in skin friction drag for an adverse pressure gradient flow were probably first observed in the total drag measurements of McCormick and Bhattacharyya.[1] For their configuration 5, wire windings were started at an X/L of 0.42 and covered only the aft 44% of the hull. The region covered by the windings and hence the hydrogen bubbles was entirely within the adverse pressure gradient region predicted for their body shape. At their lowest turbulent Reynolds number, their total drag reduction was the order of 40%. Taking account of the area covered by bubbles then, their data suggest almost complete skin friction suppression. In addition, there was no indication that their

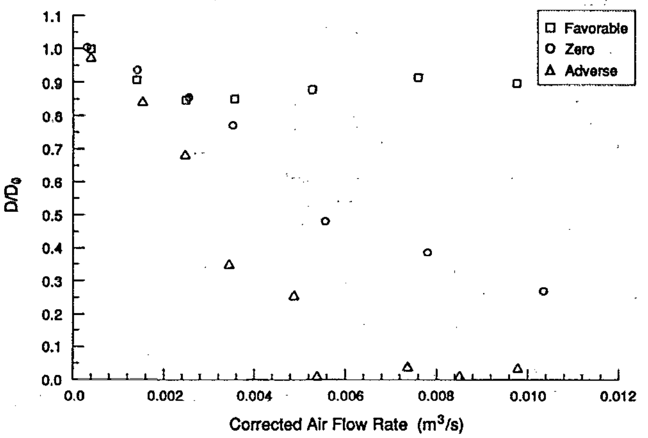

FIG. 7. Drag ratio versus corrected air flow rate for each pressure gradient at $U_\infty = 10.7$ m/sec.

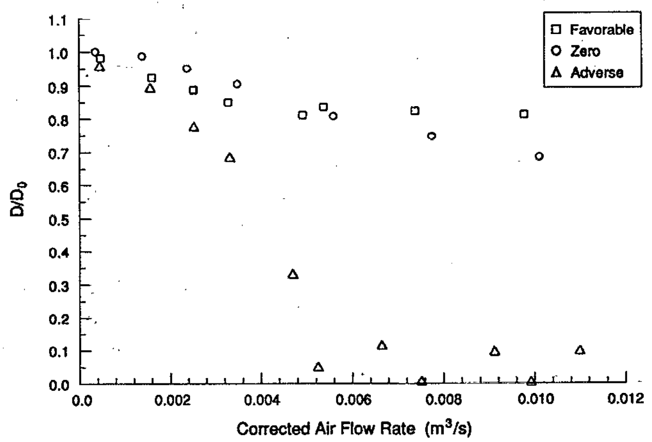

FIG. 9. Drag ratio versus corrected air flow rate for each pressure gradient at $U_\infty = 16.8$ m/sec.

bubble flow rolls up at low speeds. This tends to confirm our observation that adverse pressure gradients inhibit the roll-up phenomenon.

IV. CONCLUSIONS

In the current study, we have shown that weak, applied axial pressure gradients have a strong influence on the microbubble drag reduction phenomenon. The presence of a favorable gradient strongly inhibits the drag reduction mechanism, while separation of the boundary layer is induced at low levels of gas injection for an applied adverse gradient.

A comparison of the balance data against spatial integrations of the local skin friction suggest that the balance is working well for each gradient in the absence of bubble injection. Pressure measurements on the surface of the balance section indicate, in agreement with the work of Deutsch and Castano,[9] that the injection of bubbles does not change the axial pressure gradient or the symmetry of the flow. When taken in combination, these measurements give us some reasonable confidence that the drag measurements in the presence of gas injection are reliable. Moreover for the case in which the drag measurements may be directly checked—that is, the case of separation induced by an adverse gradient—the balance results show good agreement with the flow visualization results.

The sensitivity of the drag reduction mechanism to the application of weak (at least, from the point of view of pure liquid properties) axial pressure gradients was not an anticipated result. Our simple, working hypothesis for microbubble drag reduction has been that the bubble–liquid mixture acts as a high-viscosity fluid additive (low density, high absolute viscosity) that effectively reduces the turbulent Reynolds number and suppresses the small-scale turbulence. Near the buffer region, where the small-scale turbulence scales are, in fact, the production scales, the production of turbulence is quelled and moved farther from the wall. This acts, in effect, like an increase in sublayer thickness.

Computational[12] and experimental studies[8] have supported this hypothesis. These studies indicate that, to be effective, the bubbles must reside above the (pure liquid) sublayer and below a y^+ on the order of 100. In our experiments, at a free-stream speed of 10 m/sec, this restricts the vertical range of effectiveness of the bubbles to between 20 and 250 μm above the surface. Clearly then, the trajectories of the bubbles are of great importance in determining the drag reduction. It seems fair to speculate that the applied pressure gradient, the action of which may be two orders of magnitude more influential on the near-wall gas/liquid mixture than on the outer liquid boundary layer, may change the gas cloud trajectory significantly. In particular, one might anticipate that the favorable gradient would suppress the turbulent mixing necessary to move the bubble cloud off the wall and out of the sublayer, while the opposite would be true for the adverse pressure gradient. Simple computations of bubble trajectories, as undertaken by Pal *et al.*,[20] for example, might be of considerable value in testing such speculations.

The substantial effect of the applied pressure gradients on the drag reduction results highlights the importance of the location of the bubbles within the boundary layer. Although Merkle and Deutsch,[13] for example, have noted that the ratio of gas to total volume in the boundary layer is an effective way to correlate the high velocity drag reduction data for any given microbubble experiment, such a normalization would not be effective here. Great care must be taken then in extrapolating the existing data to full-scale models, in particular, when the full-scale model incorporates a change in relative geometry. On a more optimistic note, the large skin friction reduction for the adverse pressure gradient case at relative low values of gas injection may prove to be useful. It would seem that, for some applications, body shaping may reduce the gas flow requirements for microbubble skin friction reduction quite substantially. In a similar manner, body shaping to induce an adverse pressure gradient may suppress the roll-up phenomenon and make microbubble drag reduction more applicable to low-speed applications.

ACKNOWLEDGMENTS

This work was sponsored by the Office of Naval Research under Contract No. N00014-87-K-0196. The technical monitor was Mr. James A. Fein.

[1]M. E. McCormick and R. Bhattacharyya, Nav. Eng. J. **85**, 11 (1973).
[2]G. S. Migirenko and A. R. Evseev, Novosibirsk Nauka (1974) (Translated from Russian).
[3]Y. N. Dubnischev, E. R. Evseev, V. S. Sobolev, and E. N. Utkin, J. Appl. Mech. Tech. Phys. **16**, 114 (1975).
[4]V. G. Bogdevich and A. R. Evseev, *Investigations of Boundary Layer Control*, edited by S. S. Kutateladze and G. S. Migirenko (Thermophysics Institute, Novosibirsk, 1976).
[5]V. G. Bogdevich and A. G. Maliuga, *Investigations of Boundary Layer Control*, edited by S. S. Kutateladze and G. S. Migirenko (Thermophysics Institute, Novosibirsk, 1976).
[6]N. K. Madavan, S. Deutsch, and C. L. Merkle, Phys. Fluids **27**, 356 (1974a).
[7]N. K. Madavan, S. Deutsch, and C. L. Merkle, J. Fluid Mech. **156**, 237 (1985).
[8]S. Pal, C. L. Merkle, and S. Deutsch, Phys. Fluids **31**, 744 (1988).
[9]S. Deutsch and J. Castano, Phys. Fluids **29**, 3590 (1986).
[10]S. Deutsch and S. Pal, Phys. Fluids A **2**, 2140 (1990).
[11]H. H. Legner, Phys. Fluids **27**, 2788 (1984).
[12]N. K. Madavan, C. L. Merkle, and S. Deutsch, Trans. ASME **107**, 370 (1985).
[13]C. L. Merkle and S. Deutsch, *Lecture Notes in Engineering*, edited by M. Gad-el-Hak (Springer-Verlag, New York, 1989), Vol. 46.
[14]S. Pal, S. Deutsch, and C. L. Merkle, Phys. Fluids A **1**, 1360 (1989).
[15]S. Pal and S. Deutsch (private communication).
[16]W. C. Zierke and S. Deutsch, Applied Research Laboratory Report No. ARL/PSU TM 85-85 (Pennsylvania State University, University Park, PA, 1985).
[17]S. J. Kline, W. C. Reynolds, F. A. Schaub, and P. W. Runstadler, J. Fluid Mech. **30**, 741 (1967).
[18]G. L. Mellor, J. Fluid Mech. **24**, 255 (1966).
[19]D. M. McEligot and H. Ecklemann, Westinghouse Technical Report No. WNSD/hydro-90-03, July, 1990.
[20]S. Pal, S. Deutsch, and C. L. Merkle, 29th Aerospace Sciences Meeting, Reno, Nevada, 7–10 January 1991, AIAA Paper No. 91-0517.